

## Double Hysteresis Loops in Proper Uniaxial Ferroelectrics

I. Zamaraitė,<sup>1</sup> R. Yevych,<sup>2,\*</sup> A. Dziaugys,<sup>1</sup> A. Molnar,<sup>2</sup> J. Banys,<sup>1</sup> S. Svirskas,<sup>1</sup> and Yu. Vysochanskii<sup>2</sup>

<sup>1</sup>*Faculty of Physics, Vilnius University, Saulėtekio 9, 10222 Vilnius, Lithuania*

<sup>2</sup>*Institute for Solid State Physics and Chemistry, Uzhgorod University, Pidgirna Str. 46, Uzhgorod 88000, Ukraine*



(Received 12 April 2018; revised manuscript received 25 June 2018; published 10 September 2018)

In bulk proper uniaxial ferroelectrics, double antiferroelectriclike hysteresis loops are observed in the case of  $\text{Sn}_2\text{P}_2\text{S}_6$  crystal. The quantum-anharmonic-oscillator model is proposed for the description of such a polarization-switching process. This phenomenon is related to the three-well local potential of the spontaneous-polarization fluctuations at a distinctive negative ratio of coupling constants that correspond to intersite interaction in the given sublattice and interaction between two sublattices of the modeled  $\text{Sn}_2\text{P}_2\text{S}_6$  crystal structure. The data obtained can be used for the development of multilevel-cell-type memory technology.

DOI: 10.1103/PhysRevApplied.10.034017

### I. INTRODUCTION

With the development of modern information technology, human requirement is needed for ever-larger volumes of information storage. Due to the fact that the technological norms for reducing the size of memory cells are gradually approaching the limitations imposed by physical laws, memory manufacturers are looking for ways out of this situation. One of the methods for increasing the density of information storage is the use of memory cells with several logical states. In such systems, several bits of information are stored in one cell. Prominent examples of this approach are the multilevel-cell and triple-level cell types of flash memory [1]. However, flash technology has a number of drawbacks [2], which lead to the search for new types of memory cells. One of the candidates for the role of the nonvolatile universal memory of the future is ferroelectric memory (Fe-RAM) [3]. As it turns out, in these memory cells it is also possible to store several bits of information [4–6]. However, the practical implementation of such systems is only at the level of theoretical calculations.

Our results demonstrate the principal possibility of the application of monocrystalline materials as media for multilevel memory cells. In this paper, we propose the use of a room-temperature proper uniaxial ferroelectric semiconductor,  $\text{Sn}_2\text{P}_2\text{S}_6$ , as an active material of a ferroelectric memory cell. The three-well local potential for the spontaneous-polarization fluctuations [7] allows one cell to store several bits of information. This makes it possible

to create on its base not only memory cells but also non-Boolean information systems.

In  $\text{Sn}_2\text{P}_2\text{S}_6$  crystals, the second-order phase transition from the paraelectric phase ( $P2_1/n$ ) to the ferroelectric phase ( $Pn$ ) occurs at  $T_0 \approx 338$  K. At room temperature, spontaneous polarization is oriented in the (010) monoclinic symmetry plane near the [100] direction [8]. The origin of the spontaneous polarization is related to the electron lone-pair stereoactivity of the  $\text{Sn}^{2+}$  cations together with the  $\text{P}^{4+} + \text{P}^{4+} \longleftrightarrow \text{P}^{3+} + \text{P}^{5+}$  valence fluctuations inside the  $(\text{P}_2\text{S}_6)^{4-}$  anions [7,9,10], which, on the whole, can be considered in the frame of the second-order Jahn-Teller effect [11]. The thermodynamics of this mixed “displacive—order/disorder” continuous transition can be described using the Blume-Emery-Griffiths model [12,13], which considers the possibility of thermal fluctuations between three values of pseudospins (“−1,” “0,” and “+1”) in a local three-well potential. This model predicts the possibility of metastable nonpolar states inside the ferroelectric phase at  $T < T_0$ . By Monte Carlo simulations with an effective Hamiltonian, which is constructed on the basis of a frozen-phonon approximation, a high probability of a zero value for pseudospins inside the ferroelectric phase of  $\text{Sn}_2\text{P}_2\text{S}_6$  crystal is found [7]. Experimentally, by piezoelectric microscopy, inclusions of nonpolar “paraelectric regions” at  $T < T_0$  have been directly observed [14].

It is natural to expect the possibility of unusual switching of spontaneous polarization by an external electric field in the case of proper ferroelectric  $\text{Sn}_2\text{P}_2\text{S}_6$  in a “two-step” manner—from one side well of the local potential into the central well and then further into another side well. The metastable central-well state during the switching process

\*ruslan.yevych@uzhnu.edu.ua

can be reflected as the appearance of double hysteresis loops.

In this paper, we present the results of hysteresis-loop investigations for  $\text{Sn}_2\text{P}_2\text{S}_6$  ferroelectrics. It is found that double loops can be observed in a wide temperature interval of the ferroelectric phase. The conditions for the observation of “ordinary” ferroelectric loops are determined. Also, the influence of the crystal-lattice defects that appear upon the partial substitution of tin by lead, or of sulfur by selenium, is investigated. It is found that defects destroy double hysteresis loops in  $\text{Sn}_2\text{P}_2\text{S}_6$ .

The quantum-anharmonic-oscillator (QAO) model is developed for the description of double hysteresis loops in proper uniaxial ferroelectrics. This model is based on the description of a temperature-pressure phase diagram for  $\text{Sn}_2\text{P}_2\text{S}_6$  ferroelectrics [10] taking account of the pressure flattening of the side wells in the local three-well potential. The “ferroelectric” and “antiferroelectriclike” solutions of the developed model demonstrate the possibility of the realization of “ordinary” and “double” hysteresis loops in  $\text{Sn}_2\text{P}_2\text{S}_6$  ferroelectrics.

## II. EXPERIMENTS AND THEORETICAL DESCRIPTION

For the experimental investigations, crystals are grown from liquid by the Bridgeman method using stoichiometric amounts of chemical elements Sn, P, and S with a purity of 99.9999%. Such technology provides the samples with small low-frequency dielectric losses related to the hole conductivity of these samples, which is mostly determined by the compensation processes between the acceptor vacancies of the tin and the donor vacancies of the sulfur ions [15]. The investigated samples are characterized by XPS spectroscopy as previously described [16] and by x-ray diffraction performed with a DRON-4 diffractometer, using Cu-K $\alpha$  radiation. Their diffraction patterns are similar to those observed for samples grown by the vapor-transport technique (see, e.g., Fig. 1). All this ensures a good crystal quality as well as the absence of different phases.

Silver paste is used for the electrodes at the polar cuts of the plate shape samples, with typical dimensions of about  $3 \times 5 \times 5 \text{ mm}^3$ . The ferroelectric hysteresis ( $P$ - $E$ ) loops are measured by an aixACCT TF Analyzer 2000 ferroelectric measurement system (aixACCT Co., Aachen, Germany) equipped with a high-voltage amplifier. The bipolar triangular voltage wave is applied on the sample for the measurement of the polarization. The frequency of the signal is varied in the range of 3–30 Hz. The polarization is determined from the experimental data of the electrical current flowing through the sample. Dielectric characterization is performed with a HP4284 precision LCR meter at temperatures from 400 to 100 K during the cooling cycle,

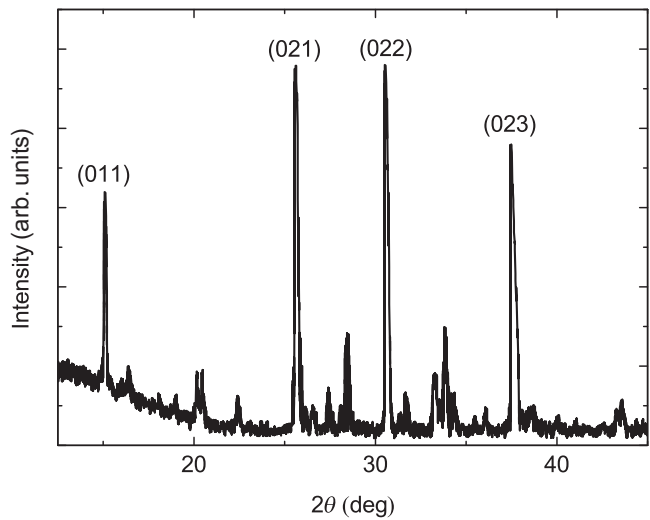


FIG. 1. An example of a diffraction pattern for  $\text{Sn}_2\text{P}_2\text{S}_6$  crystal at room temperature.

at a rate of about 1 K/min, and at frequencies ranging from 20 to 1 MHz.

As can be seen in Fig. 2, the second-order phase transition is manifested by a sharp peak in the temperature dependencies of the dielectric susceptibility near  $T_0$  (for both the real and the imaginary parts). The dielectric losses in the polar phase have a sufficiently high value but they decrease rapidly below 260 K.

For an as-grown  $\text{Sn}_2\text{P}_2\text{S}_6$  sample below  $T_0$ , the hysteresis loops have a double kind of shape [Figs. 3(a)–3(d)]. At zero field, the spontaneous polarization is very small ( $< 1 \mu\text{C}/\text{cm}^2$ ) but it reaches  $8 \mu\text{C}/\text{cm}^2$  upon an increase of the electric-field amplitude to 6 kV/cm for  $T = 318 \text{ K}$ . As is evident, the double hysteresis loops are

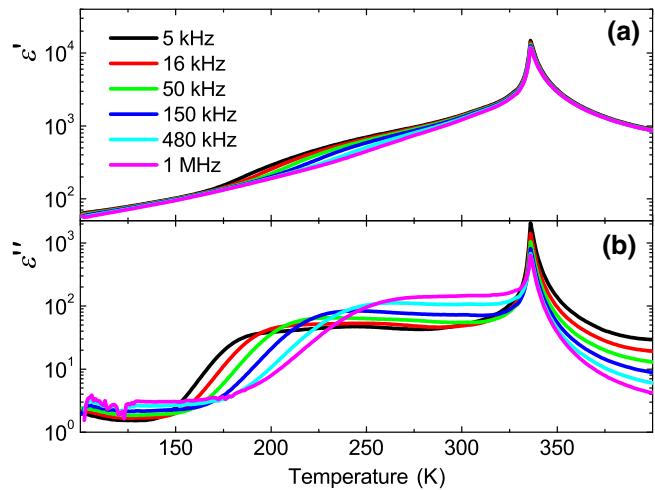


FIG. 2. The temperature dependencies of (a) the real and (b) the imaginary parts of the dielectric susceptibility for  $\text{Sn}_2\text{P}_2\text{S}_6$  crystal at different frequencies of applied field.

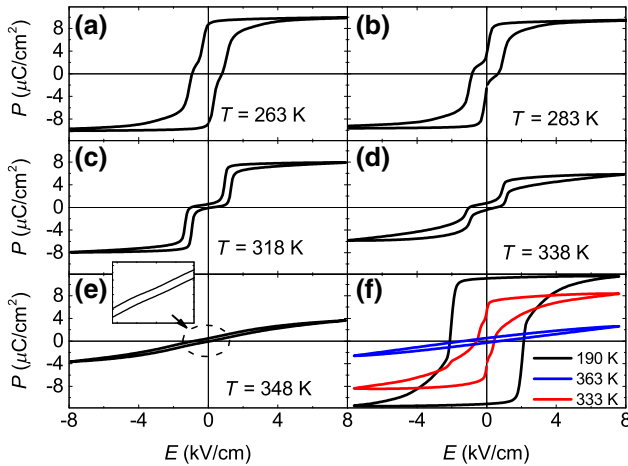


FIG. 3. (a)–(e) The  $P$ - $E$  hysteresis for an as-grown  $\text{Sn}_2\text{P}_2\text{S}_6$  sample at different temperatures. (f) The  $P$ - $E$  hysteresis loops for a  $\text{Sn}_2\text{P}_2\text{S}_6$  sample that has been annealed in the paraelectric phase at 383 K for 2 h and then cooled to 190 K.

connected by two lines crossing the origin point for the  $P$ - $E$  graph. Such a peculiarity is related to the electrical conductivity of the investigated samples. For the same reason, the shape of the loops in the paraelectric phase, above 338 K, is found to be deformed ellipse-like [Fig. 3(e)]. Upon cooling below 283 K, the hysteresis loops take up the usual ferroelectric shape with a spontaneous-polarization value near  $10 \mu\text{C}/\text{cm}^2$  and a coercive field of about 1 kV/cm.

After the  $\text{Sn}_2\text{P}_2\text{S}_6$  sample has been kept in the paraelectric phase at a temperature of about 373 K for 2 h and with further cooling to 190 K, ordinary ferroelectric loops are observed [Fig. 3(f)]. At the same time, the spontaneous polarization and coercive field reach values of about  $11 \mu\text{C}/\text{cm}^2$  and 2 kV/cm, respectively. However, after the sample has been kept at room temperature for a few weeks, antiferroelectriclike double loops are again observed. It should be noted that this phenomenon is repetitive for different samples. Obviously, the balance between the ferroelectric and antiferroelectric states is determined by the long-time relaxation processes in the electron subsystem of the  $\text{Sn}_2\text{P}_2\text{S}_6$  ferroelectric semiconductor. These findings should be subjected to further investigation.

The  $P$ - $E$  hysteresis is investigated at different switching parameters (the frequency and amplitude of the electric field). In all measurements, the double hysteresis loops demonstrate their antiferroelectriclike shape over the whole range of variation of parameters [Figs. 4(a) and 4(b)]. For example, the switching-current hysteresis is shown in Fig. 4(c) at different frequencies of the applied electric field. As expected, it has four peaks related to double hysteresis loops.

In  $(\text{Pb}_y\text{Sn}_{1-y})_2\text{P}_2\text{S}_6$  and  $\text{Sn}_2\text{P}_2(\text{Se}_x\text{S}_{1-x})_6$  mixed crystals, the usual ferroelectric loops are observed. In the elementary cell of  $\text{Sn}_2\text{P}_2\text{S}_6$  crystals, all atoms are placed

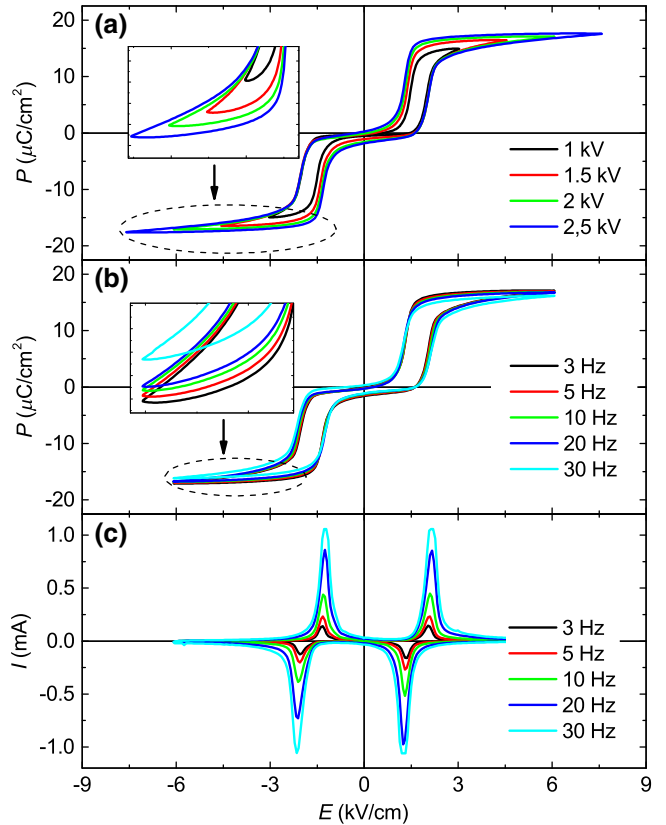


FIG. 4. The  $P$ - $E$  hysteresis loops measured in a  $\text{Sn}_2\text{P}_2\text{S}_6$  sample at room temperature with various switching parameters: (a) different voltage amplitudes at a frequency of 3 Hz; (b) different frequencies with a voltage amplitude of 2 kV. (c) The switching-current–field dependencies that are related to the hysteresis loops at a voltage amplitude of 2 kV at different frequencies.

in general positions with  $C_1$  point-group symmetry [8]. It follows that the atomic substitution increases the crystal-lattice defects and avoids the possibility of the observation of double loops.

We suppose that the observed peculiar switching in  $\text{Sn}_2\text{P}_2\text{S}_6$  ferroelectrics is determined by the local three-well potential for the spontaneous-polarization fluctuations at a specified negative ratio of intersite interactions in a given sublattice and between two sublattices of the  $\text{Sn}_2\text{P}_2\text{S}_6$  crystal structure [7,8]. The QAO model presented below describes the possibility of the realization of double (antiferroelectriclike) hysteresis loops in such proper uniaxial ferroelectrics.

In this work, we develop an enhanced QAO model that has previously been described for the investigated crystal [10]. The main difference consists in the model representation of a crystal lattice. The real crystal lattice has been described earlier as a one-dimensional chain of equivalent quantum-anharmonic oscillators. The interaction of the oscillators is described within the mean-field approach, which makes it possible to consider such a system as

one comprised of noninteracting oscillators. Therefore, the Hamiltonian of the system has the form

$$H = \sum_i (T(x_i) + V(x_i) + J\langle x \rangle x_i), \quad (1)$$

where the  $T(x_i)$  and  $V(x_i)$  are the operators of the kinetic and potential energy, respectively,  $\langle x \rangle$  is the average value of the displacement coordinate  $x_i$ , and  $J$  is the coupling constant. Here, the last term in the Hamiltonian given in Eq. (1) reflects the mean-field approach by taking the relation  $\sum_{ij} J_{ij} x_i x_j \approx \sum_i J\langle x \rangle x_i$  into account.

Suppose that we now describe the  $\text{Sn}_2\text{P}_2\text{S}_6$  crystal lattice as two interacting subsystems of oscillators. The elementary cell of  $\text{Sn}_2\text{P}_2\text{S}_6$  contains two formula units, which are related by the symmetry plane (see Fig. 5). Despite the three-dimensional structure of the  $\text{Sn}_2\text{P}_2\text{S}_6$  crystal, its lattice can be presented as two chains of equivalent sites with a local three-well potential. The shape of the local three-well potential has been determined earlier by first-principles calculations [7]. This shape can be changed by pressure or with variation of the chemical composition in mixed crystals [10]. For simplicity, the chains are completely identical and are characterized by the same local potential  $V$  for each site and coupling constant  $J_1$ . However, the interaction between oscillators from different subsystems is characterized by another coupling constant,  $J_2$ . The mean-field approach is also applied. Therefore, the total Hamiltonian  $H_t$  for such a system can be written as a sum of two Hamiltonians  $H_1$  and  $H_2$  for each  $x$  and  $y$  subsystem:

$$H_t = H_1 + H_2,$$

$$H_1 = \sum_i (T(x_i) + V(x_i) + (J_1\langle x \rangle + J_2\langle y \rangle)x_i), \quad (2)$$

$$H_2 = \sum_i (T(y_i) + V(y_i) + (J_2\langle x \rangle + J_1\langle y \rangle)y_i). \quad (3)$$

Self-consistently solving the system of Eqs. (2)–(3), we can obtain the energy levels and corresponding wave functions of the system (for details, see Ref. [10] and references therein). To investigate the influence of an external electric field  $E$  on the model system, the terms proportional to  $Ex_i$  and  $Ey_i$  should be added to Eqs. (2) and (3), respectively. Then, the order parameter, which is proportional to the sum of the average displacements of the oscillators, and other physical properties can be calculated for different temperatures.

It should be noted that the shape of the local three-well potential  $V$  is phenomenologically described by the nonlinear interaction  $A_g B_u^2$  of several low-energy optic modes of  $B_u$  symmetry with fully symmetrical  $A_g$  modes [7]. The shifts of the  $\text{Sn}^{2+}$  cations relative to the anions (Fig. 5) are accompanied by recharging and change in the covalency of the chemical bonds determining the origin of the local

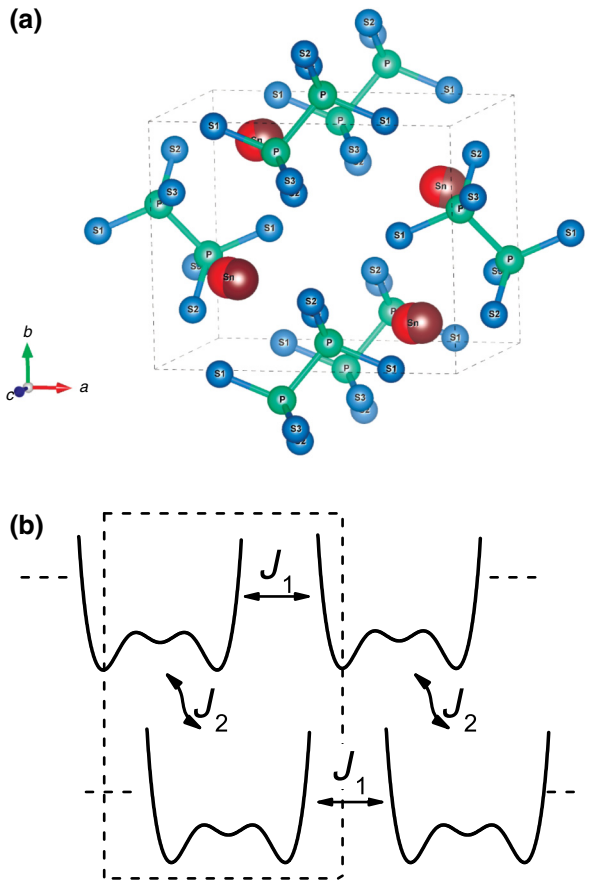


FIG. 5. (top) The crystal structure of  $\text{Sn}_2\text{P}_2\text{S}_6$ . The positions of the tin cations (large spheres) in the paraelectric and ferroelectric phases are shown by different colors. Two sublattices are presented by two formula units in a monoclinic elementary cell. (bottom) The QAO model with two chains that belong to two sublattices in the  $\text{Sn}_2\text{P}_2\text{S}_6$  crystal structure. The local dipoles in every  $\text{Sn}_2\text{P}_2\text{S}_6$  formula unit fluctuate in the three-well potential. The interaction within sublattices (chains) is determined by constant  $J_1$ , while that between sublattices (chains) is determined by constant  $J_2$ .

electric dipoles in every  $\text{Sn}_2\text{P}_2\text{S}_6$  formula unit. At the given site, the fluctuations of the pseudospin in such a local three-well potential can be related to the Hubbard-Holsstein model for systems with electronic correlations involving phononic excitation [17]. Such a description can be projected on to the Blume-Emery-Griffiths (BEG) model with three values of pseudospins (“−1,” “0,” and “+1”) and with two order parameters—dipolar with  $B_u$  symmetry and quadrupolar with  $A_g$  symmetry [18].

Upon evaluation of the QAO model parameters, the local three-well potential, which is determined by first-principles calculations [7], is taken into account. The “inter-chain” coupling constant  $J_1$  is chosen to fit the second-order phase transition temperature  $T_0 \approx 338$  K at normal pressure. Also taken into account is the fact that for  $\text{Sn}_2\text{P}_2\text{S}_6$  crystal, the ratio of interactions  $J_2/J_1 \approx -0.23$

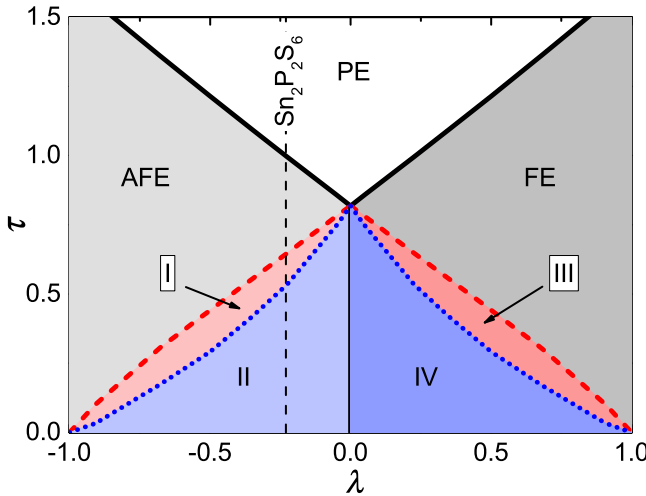


FIG. 6. The reduced-temperature-coupling-constant-ratio phase diagram for the QAO model with stable paraelectric (PE), ferroelectric (FE), and antiferroelectric (AFE) phases. The coexistence of metastable AFE and FE states can be reached upon lowering of the temperature: region I contains, in addition to the stable AFE phase, one state with FE ordering, while region II contains two FE states; region III contains, in addition to the stable FE phase, one state with AFE ordering, while region IV contains two AFE states. The thermodynamic path for the  $\text{Sn}_2\text{P}_2\text{S}_6$  crystal is highlighted by the vertical dashed line.

[8], which follows from analysis of the  $T - x$  diagram of  $\text{Sn}_2\text{P}_2(\text{Se}_x\text{S}_{1-x})_6$  mixed crystals in the axial next-nearest-neighbor Ising (ANNNI) model [19], explains the observed Lifshitz point at  $x_{LP} \approx 0.28$  and continuous transitions from the paraelectric phase into the incommensurate phase at  $x > x_{LP}$ .

Let us introduce dimensionless parameters such as the reduced temperature ( $\tau = T/T_0$ ) and the ratio of the coupling constants  $\lambda = J_2/J_1$ . The calculated in described QAO model  $\tau$ - $\lambda$  phase diagram is shown in Fig. 6. It contains paraelectric (PE), ferroelectric (FE), and antiferroelectric (AFE) phases, and four regions (I–IV) with metastable states. There are two points,  $\lambda = 1$  and  $\lambda = -1$ , where no metastable regions occur, and pure FE and AFE phases, respectively, can be observed. Also, in the case of  $\lambda = 0$  (no interaction between different chains), FE or AFE phases can be realized with equal probability. The  $\lambda = -0.23$  point on the phase diagram can be associated with the model parameters for the  $\text{Sn}_2\text{P}_2\text{S}_6$  crystal. For such parameters, the AFE phase appears at cooling below  $T_0$ . But inside the AFE phase, metastable FE states are also predicted (Fig. 6). For this case, the temperature dependencies of the total reduced polarization  $\rho$  (where  $\rho = P/P_0$  and  $P_0$  is a polarization in one subsystem at zero temperature for a stable solution) for all solutions are presented in Fig. 7. The contributions from different chains to the total polarization are shown in the insets. As is evident, the phase transition from the PE phase to the AFE phase at  $\tau = 1$  is a continuous transition, and additional metastable

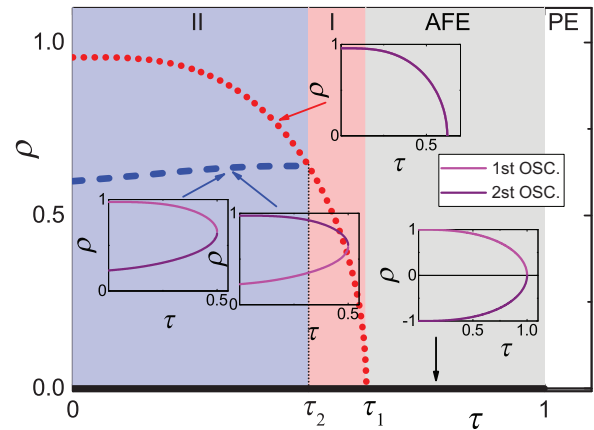


FIG. 7. The temperature dependencies of the total reduced-order parameters for all solutions in the case of  $\lambda = -0.23$ . The thick black line corresponds to the order parameter of the AFE phase, which appears continuously at  $\tau \leq 1$ ; the red dotted line corresponds to the continuous appearance of the FE phase at  $\tau \leq \tau_1 \approx 0.62$ ; and the blue dashed line corresponds to the discontinuous appearance of the FE phase at  $\tau \leq \tau_2 \approx 0.5$ . The magenta and purple lines in the insets correspond to contributions to the total polarization from the first and the second subsystem, respectively.

states with FE ordering of oscillator displacements appear continuously at  $\tau = \tau_1$  and discontinuously at  $\tau = \tau_2$ .

The calculated dependence of the reduced polarization  $\rho$  versus the reduced electric field  $\xi$  dependence (where  $\xi = E/E_0$  and  $E_0$  is a coercive field at zero temperature) for different temperatures demonstrates several branches of stable and metastable solutions (Fig. 8). At zero temperature on a hysteresis loop, for example, there are three stable solutions, for which the polarization increases with an increase in the applied field, and three metastable solutions, for which the polarization decreases with an increase in the applied field. These solutions demonstrate the possibility of the observation of double hysteresis loops for proper uniaxial ferroelectrics  $\text{Sn}_2\text{P}_2\text{S}_6$  with a three-well local potential for spontaneous-polarization fluctuations and at a negative ratio of interactions inside and between the structure sublattices.

Finally, we turn to the interesting question of why annealing in the paraelectric phase destroys the conditions for the observation of double loops upon cooling below  $T_0$ . As we mentioned earlier, for a  $\text{Sn}_2\text{P}_2\text{S}_6$  ferroelectric semiconductor, spontaneous polarization is related to the stereoactivity of the tin cations and the valence fluctuations of the phosphorous cations. Recharging occurs and the changes in the covalence of the chemical bonds can be presented as small-hole polar formation in a given  $\text{SnPS}_3$  structural group and the appearance of small electron polarons in the nearest  $\text{SnPS}_3$  structural group [10]. The local dipole in the  $\text{Sn}_2\text{P}_2\text{S}_6$  formula unit can be originated by a polaronic exciton, and the ferroelectric phase can be

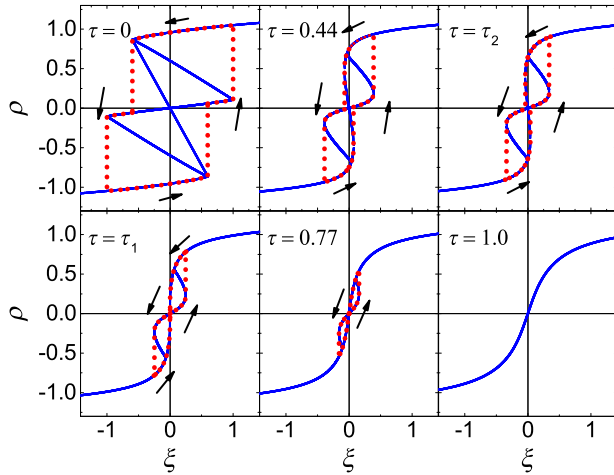


FIG. 8. The calculated dependencies of the polarization from the external electric field at different temperatures for the case of  $\lambda = -0.23$  (blue lines). Possible hysteresis loops for each temperature are shown by the red dotted lines.

characterized as a coherent state of polaronic excitons. At heating above  $T_0$ , free carriers are thermally excited. They can be trapped at the lattice imperfections, producing dipole defects in the paraelectric phase and, obviously, these prevent the observation of double dielectric loops below  $T_0$ .

### III. CONCLUSIONS

Polarization switching in the form of double hysteresis loops in bulk proper uniaxial ferroelectrics is observed in the case of  $\text{Sn}_2\text{P}_2\text{S}_6$  crystal. Such a peculiarity is related to the three-well shape of the local potential for spontaneous-polarization fluctuations, which determine the possibility of the existence of metastable nonpolar regions below the second-order phase-transition temperature  $T_0 \approx 338$  K. The origin of the spontaneous polarization is determined by changes in the chemical bonding that can be presented as a second-order Jahn-Teller effect based on the electron lone-pair stereoactivity of the  $\text{Sn}^{2+}$  cations and the  $\text{P}^{4+} + \text{P}^{4+} \longleftrightarrow \text{P}^{3+} + \text{P}^{5+}$  valence fluctuations of the phosphorous cations. An enhanced quantum-anharmonic-oscillator model is proposed, which considers a negative ratio of the interactions inside and between the sublattices in the  $\text{Sn}_2\text{P}_2\text{S}_6$  crystal. This model can explain the coexistence of ferroelectric and antiferroelectric hysteresis loops in  $\text{Sn}_2\text{P}_2\text{S}_6$  crystals, an observation that can be used for the development of the multilevel-cell type of memory technology.

- [2] J. S. Meena, S. M. Sze, U. Chand, and T.-Y. Tseng, Overview of emerging nonvolatile memory technologies, *Nanoscale Res. Lett.* **9**, 526 (2014).
- [3] B.-E. Park, H. Ishiwara, M. Okuyama, S. Sakai, and S.-M. Yoon, *Ferroelectric-Gate Field Effect Transistor Memories: Device Physics and Applications* (Springer, Dordrecht, 2016).
- [4] L. Baudry, I. Lukyanchuk, and V. M. Vinokur, Ferroelectric symmetry-protected multibit memory cell, *Sci. Rep.* **7**, 42196 (2017).
- [5] A. G. Boni, C. Chirila, I. Pasuk, R. Negrea, I. Pintilie, and L. Pintilie, Steplike Switching in Symmetric  $\text{PbZr}_{0.2}\text{Ti}_{0.8}\text{O}_3/\text{CoFeO}_4/\text{PbZr}_{0.2}\text{Ti}_{0.8}\text{O}_3$  Heterostructures for Multistate Ferroelectric Memory, *Phys. Rev. Appl.* **8**, 034035-1 (2017).
- [6] G. A. Boni, L. D. Filip, C. Chirila, I. Pasuk, R. Negrea, I. Pintilie, and L. Pintilie, Multiple polarization states in symmetric ferroelectric heterostructures for multi-bit non-volatile memories, *Nanoscale* **9**, 19271 (2017).
- [7] K. Z. Rushchanskii, Yu. M. Vysochanskii, and D. Strauch, Ferroelectricity Nonlinear Dynamics, and Relaxation Effects in Monoclinic  $\text{Sn}_2\text{P}_2\text{S}_6$ , *Phys. Rev. Lett.* **99**, 207601-1 (2007).
- [8] Yu. M. Vysochanskii, T. Janssen, R. Currat, R. Folk, J. Banys, J. Grigas, and V. Samulionis, *Phase Transitions in Ferroelectric Phosphorous Chalcogenide Crystals* (Vilnius University Publishing House, Vilnius, 2006).
- [9] K. Glukhov, K. Fedyo, J. Banys, and Yu. Vysochanskii, Electronic structure and phase transition in ferroelectric  $\text{Sn}_2\text{P}_2\text{S}_6$  crystal, *Int. J. Mol. Sci.* **13**, 14356 (2012).
- [10] R. Yevych, V. Haborets, M. Medulych, A. Molnar, A. Kohutych, A. Dziaugys, Ju. Banys, and Yu. Vysochanskii, Valence fluctuations in  $\text{Sn}(\text{Pb})_2\text{P}_2\text{S}_6$  ferroelectrics, *Low Temp. Phys.* **42**, 1155 (2016).
- [11] I. B. Bersuker, Pseudo-Jahn-Teller Effect—A two-state paradigm in formation, deformation, and transformation of molecular systems and solids, *Chem. Rev.* **113**, 1351 (2013).
- [12] M. Blume, V. J. Emery, and R. B. Griffiths, Ising model for the  $\lambda$  transition and phase separation in  $\text{He}^3\text{-He}^4$  mixtures, *Phys. Rev. A* **4**, 1071 (1971).
- [13] C. Ekiz, M. Keskin, and O. Yalcin, Metastable and unstable states of the Blume-Capel model obtained by the cluster variation method and the path probability method, *Physica A* **293**, 215 (2001).
- [14] D. A. Kiselev, K. Z. Rushchanskii, M. D. Malinkovich, Y. N. Parkhomenko, and Yu. M. Vysochanskii, Theoretical prediction and direct observation of metastable non-polar regions in domain structure of  $\text{Sn}_2\text{P}_2\text{S}_6$  ferroelectrics with triple-well potential, *Ferroelectrics* **438**, 55 (2012).
- [15] Yu. Vysochanskii, K. Glukhov, M. Maior, K. Fedyo, A. Kohutych, V. Betsa, I. Prits, and M. Gurzan, Ferroelectric and semiconducting properties of  $\text{Sn}_2\text{P}_2\text{S}_6$  crystals with intrinsic vacancies, *Ferroelectrics* **418**, 124 (2011).
- [16] J. Grigas, E. Talik, V. Lazauskas, Yu. M. Vysochanskii, R. Yevych, M. Adamiec, and V. Nelkinas, XPS of electronic structure of ferroelectric  $\text{Sn}_2\text{P}_2\text{S}_6$  crystals, *Ferroelectrics* **378**, 70 (2009).
- [17] M. Fabrizio, A. O. Gogolin, and A. A. Nersesyan, From Band Insulator to Mott Insulator in One Dimension, *Phys. Rev. Lett.* **83**, 2014 (1999).

[1] G. Torelli, M. Lanzoni, A. Manstretta, and B. Ricco, in *Flash Memories* (Springer, Boston, 1999), p. 361.

- [18] T. M. Rice and L. Sneddon, Real-Space and  $\vec{k}$ -Space Electron Pairing in  $\text{BaPb}_{1-x}\text{Bi}_x\text{O}_3$ , [Phys. Rev. Lett. \*\*47\*\*, 689 \(1981\)](#).
- [19] W. Selke, Ising model with isotropic competing interactions in the presence of a field: A tricritical-Lifshitz-point realization, [Phys. Rep. \*\*170\*\*, 213 \(1988\)](#); T. Janssen, in *Incommensurate Phases in Dielectrics, I. Fundamentals*, edited by R. Blinc and A. P. Levanyuk (North-Holland Physics Publishing, Amsterdam, 1986); M. C. Barbosa, Ising model with isotropic competing interactions in the presence of a field: A tricritical-Lifshitz-point realization, [Phys. Rev. E \*\*48\*\*, 1744 \(1993\)](#).